Journal of CO2 Utilization 74 (2023) 102535

Contents lists available at ScienceDirect

Journal of CO2 Utilization

journal homepage: www.elsevier.com/locate/jcou

Direct hydrogenation of carbon dioxide to methanol: Systematic generation of multi-stage designs

Magne Hillestad

Department of Chemical Engineering, Norwegian University of Science and Technology (NTNU), NO-7491Trondheim, Norway

ARTICLE INFO

Keywords:
Direct hydrogenation of CO_2
Green methanol
Systematic staging
Path optimization
CO_2 utilization

ABSTRACT

Commercial methanol catalysts based on $Cu/ZnO/Al_2O_3$ are less effective applied to direct hydrogenation of CO_2 to methanol. The main reason is that the catalyst deactivation increases with the water pressure and temperature, and from stoichiometry, water formation is equal to the CO_2 consumption. Here, the focus is on how the process can be designed to reduce this problem. Multi-stage reactor designs with inter-condensation of water and methanol will reduce the water pressure. Several optimal designs are generated with the use of a path optimization method to maximize the methanol production per pass with the use of the least possible reaction volume and hydrogen. Based on a published kinetic model, the optimal volume stage distribution, coolant temperature, and fluid mixing are found. Two configurations of the tail gas treatment are investigated, a once-though and a recycle configuration. A three-stage reactor design with recycling of the tail gas is found to be the better configuration. High CO_2-conversion per pass and a low recycle ratio are obtained. Rigorous process simulations of the most promising designs are made to verify that the pressure drop, temperature peaks, and water pressure are good. The maximum water pressure is low. A shell and tube boiling water type reactor design is selected. For a 10 t h^{-1} plant, all tubes of all three stages can be located in the same shell.

1. Introduction

Carbon capture and utilization (CCU) is one of several measures to mitigate the greenhouse effect. The CO_2 can be captured from a point source such as a power plant, direct from the air, or the ocean. With hydrogen produced from renewable or low-carbon energy via electrolysis of water, can re-energize CO_2 to energy products. One possible synthesis is the hydrogenation of CO_2 with hydrogen to produce methanol. Patterson et al. [1] presented a concept with floating solar islands to recycle CO_2 captured from the ocean to produce green methanol.

Hydrogenation of CO_2 to methanol will produce more water than hydrogenation of CO. The stoichiometry shows that water formation is equal to the consumption of CO_2. Commercial methanol catalysts based on Cu combined with ZnO are less effective with a CO_2-rich feed. This is because water accelerates the crystallization of Cu and ZnO particles, resulting in rapid sintering and deactivation. In addition, other hydrogenated products such as higher alcohols and hydrocarbons are often formed along with methanol [2]. In addition to water, increased temperature will also increase the sintering effect. Thermodynamically, CO_2 is a more stable molecule than CO, therefore a gas consisting of merely CO_2 and hydrogen are less reactive than a conventional syngas.

Much research is focused on developing resilient catalysts that can tolerate high water pressures. Ren et al. [3] give a review of catalyst development to mitigate the sintering problem. The main focus here, however, is how the process can be designed to mitigate the problem of catalyst sintering and deactivation with the existing commercial catalyst. An indirect solution to reduce the problem is first to convert CO_2 and H_2 to CO and H_2O via the reversed water gas shift (rWGS) reaction, and subsequently knock out water before the syngas is fed to the methanol synthesis. The rWGS reaction is endothermic and to convert most of the CO_2 to CO, high temperatures and a separate reactor are required. This concept was suggested by Lurgi already in 1995 [4].

Several authors have studied the direct hydrogenation of CO_2 to methanol. Bansode and Urakawa [5] achieve very high CO_2 conversion per pass and high selectivity to methanol on a commercial catalyst by increasing the total pressure to 360 bar. They also applied over-stoichiometric hydrogen feed with H_2:CO_2 ratios of up to 14:1. At these conditions, the CO_2-conversion per pass reaches 95% with high selectivity to methanol. However, they did not mention the problem with sintering and deactivation. Samimi, Rahimpour, and Shariati [6], suggest a concept where the reactor path is divided into three stages. Water and methanol are condensed and extracted from the process between the stages. By removing water, the catalyst will on average “see”

E-mail address: magne.hillestad@ntnu.no.

https://doi.org/10.1016/j.jcou.2023.102535
Received 12 April 2023; Received in revised form 12 June 2023; Accepted 29 June 2023

Nomenclature

Roman symbols

a	Specific heat transfer area $a = A_{\mathrm{R}}/V_{\mathrm{R}}$, m^2 m^{-3}.
$\mathbf{x}$	State vector $\mathbf{x} = [\omega_1, \cdots\omega_n, \theta]^T$.
J	The objective function to be maximized.
D	The denominator of the rate expressions, defined in Eqn. (24).
u_{M}	The mixing design function.
u_{H}	The heat removal design function, $u_{\mathrm{H}} = \sigma\beta$.
u_{F}	The feed design function, $u_{\mathrm{F}} = \sigma\alpha$.
u_{S}	The separation design function.
N_{st}	Number of stages.
w_1	The relative cost of increasing the reaction volume.
w_2	The relative cost of increasing the extra hydrogen feed.
W_0	The make-up gas feed flow rate, kg s^{-1}.
s_i	The degree of separation of component i after a stage, $s_i \in [0,1]$.
$W_{\mathrm{H_2}}$	The feed rate of extra hydrogen, kg s^{-1}.
V_{R}	The total reaction volume, m^3.
$X_{\mathrm{CO_2}}$	The conversion of CO_2 per pass.
$\widetilde{\mathbf{R}}$	Vector of reaction rates $\widetilde{\mathbf{R}}(\mathbf{x}) = [\widetilde{R}_1, \ldots, \widetilde{R}_n, \widetilde{R}_\theta]^T$.
$\widetilde{R}_i$	Mass based component reaction rate $\widetilde{R}_i = M_i \sum_j \nu_{i,j} r_j$, kg m^{-3} s^{-1}.
$\widetilde{R}_\theta$	Temperature rate $\widetilde{R}_\theta = (\sum_j r_j(-\Delta H)_j)/(c_{\mathrm{p}} T_{\mathrm{ref}})$, kg m^{-3} s^{-1}.
R_i	Molar based component reaction rate $R_i = \sum_j \nu_{i,j} r_j$, kmol m^{-3} s^{-1}.
$\widetilde{\mathbf{J}}$	The Jacobian, $\widetilde{\mathbf{J}} = \partial\widetilde{\mathbf{R}}/\partial\mathbf{x}$.
r_j	Reaction rate of reaction $j \in \{\mathrm{A, B, C}\}$, kmol s^{-1} m^{-3}.
r'_j	Reaction rate of reaction $j \in \{\mathrm{A, B, C}\}$, kmol s^{-1} kg$_{\mathrm{cat}}^{-1}$.
U	The overall heat transfer coefficient, kW K^{-1} m^{-2}.
v	The superficial gas velocity, m s^{-1}.
q	Volumetric flow rate, m^3 s^{-1}.
T	Temperature along the path,˚C.

Greek symbols

ξ	Path length, $\xi = V/V_{\mathrm{R}}$.
ω	The mass fraction of each component.
θ	Dimensionless temperature, $\theta = (T - T_{\mathrm{ref}})/T_{\mathrm{ref}}$.
σ	The total reaction volume over the make-up feed, $\sigma = V_{\mathrm{R}}/W_0$, m^3 s kg^{-1}.
γ	The relative mass flow along the path, $\gamma = W/W_0$.
β	The heat transfer design function, $\beta = Ua/c_{\mathrm{p}}$, kg m^{-3} s^{-1}.
α	The feed distribution design function, kg m^{-3} s^{-1}.

lower water pressure and catalyst sintering will be reduced. Also, by removing the products, the equilibrium is shifted and the conversion per pass can be increased. With their configuration, they could achieve a CO_2-conversion of approximately 65% at 77 bar. Lacerda de Oliveira Campos et al. [7] have considered a similar three-stage reactor concept and have made a techno-economic comparison of a three-stage and a one-stage configuration. Their simulations indicate a CO_2-conversion per pass of 54% at 70 bar for a three-stage design. All three works [5–7] are based on a $Cu/ZnO/Al_2O_3$ catalyst. A similar concept is proposed by Air Liquide [8,9] that is called second generation CO_2-based methanol. They use a new reactor concept, that is earlier applied as heat exchangers, called a pillow plate reactor.

Also in this work, a multi-stage concept of the methanol synthesis process is applied. To increase the CO_2-conversion per pass, extra hydrogen is added beyond the stoichiometric requirement. The combined effect of multi-staging with inter-condensation and high hydrogen concentration is high CO_2-conversion per pass and low water pressure. The maximum water pressure in the best cases is the same as with a conventional methanol synthesis of syngas.

A systematic method is applied to determine the optimal total reaction volume, the size distribution of stages, the amount of additional hydrogen, the coolant temperature, and the fluid mixing at each stage are subject to optimization. Close to 100% CO_2-conversion per pass is possible even at moderate pressures. For most cases shown here, we set a target of the CO_2-conversion per pass to be at least 95% as a constraint.

Two alternative configurations for treating the tail gas from the last stage are considered. One is a once-through configuration where the excess hydrogen of the tail gas is recovered with a pressure swing adsorption. The other alternative is where the major part of the tail gas is recycled without component separation. The latter is evaluated to be a better option.

2. Methods

2.1. The path optimization method

The theoretical basis of the path optimization method is developed and described in a previous article [10]. However, here with some additions and changes that are implemented later. The independent variable, the reaction path length is the dimensionless reaction volume, $\xi = V/V_{\mathrm{R}}$, where V_{R} is the total reaction volume. The reaction path is divided into a pre-selected number of stages (N_{st}). The relative size of each stage is $\Delta\xi_i$ is the volume distribution. The make-up gas mass flow rate is W_0. The total scaled reaction volume is $\sigma = V_{\mathrm{R}}/W_0$, and the relative volume distribution, and several design functions can be determined so as to maximize an objective function. The state-space model, Eqn. (1), describes how the state vector $\mathbf{x}$ changes along the path length. The state vector is a vector of component mass fractions and dimensionless temperature, $\mathbf{x} = [\omega_1, \cdots\omega_n, \theta]^T$. The total mass flow rate along the path, W, is scaled by the make-up gas flow rate, $\gamma = W/W_0$. The design function u_{M} represents the fluid mixing. When u_{M} is zero it represents segregated flow (PFR) and when $u_{\mathrm{M}} = \xi$ it represents a completely mixed fluid (CSTR). Any degree of dispersion between these two extremes is also possible to represent by the function u_{M}. The external heat transfer to or from the reactor path is given by the ratio $\beta = Ua/c_{\mathrm{p}}$ and the dimensionless design function is $u_{\mathrm{H}} = \beta\sigma$.

$$[\gamma\mathbf{I} - u_{\mathrm{M}}\sigma\widetilde{\mathbf{J}}]\cdot\frac{\mathrm{d}\mathbf{x}}{\mathrm{d}\xi} = \sigma u_{\mathrm{A}}\widetilde{\mathbf{R}}(\mathbf{x}) - u_{\mathrm{H}}\begin{bmatrix}\mathbf{0}\\ \theta - u_{\mathrm{T}}\end{bmatrix} + \delta(\xi_i, u_{\mathrm{F}}) - \delta(\xi_i, u_{\mathrm{S}}) \tag{1}$$

The vector $\widetilde{\mathbf{R}}(\mathbf{x}) = [\widetilde{R}_1, \cdots, \widetilde{R}_n, \widetilde{R}_\theta]^T$ contains the component reaction rates on a mass basis and the temperature rate $\widetilde{R}_\theta = (\sum_j r_j(-\Delta H)_j)/(c_{\mathrm{p}} T_{\mathrm{ref}})$. The rate elements all have unit kg m^{-3} s^{-1}. The matrix $\widetilde{\mathbf{J}} = \partial\widetilde{\mathbf{R}}(\mathbf{x})/\partial\mathbf{x}$ is the Jacobian.

The external feed along the path may, in principle, be continuous, given by α with unit kg s^{-1} m^{-3} and the dimensionless design function is $u_{\mathrm{F}} = \alpha\sigma$. Here, only point feeds are allowed just before each stage. Extra hydrogen is the only external feed here, $u_{\mathrm{F}} = W_{\mathrm{H_2}}/W_0$. Both the external feed u_{F} and the separation function u_{S} are indicated with Dirac delta functions in Eqn. (1). Integrating the delta function the effect of extra feed at a point is

$$\delta\gamma = \int_{\Delta\xi} u_{\mathrm{F}}\mathrm{d}\xi \tag{2}$$

$$\delta\omega_i = \frac{\delta\gamma}{\gamma + \delta\gamma}(\omega_{F,i} - \omega_i) \tag{3}$$

$$\delta\theta = \frac{\kappa\delta\gamma}{\gamma + \kappa\delta\gamma}(\theta_F - \theta) \tag{4}$$

$$\gamma \leftarrow \gamma + \delta\gamma \tag{5}$$

$$\omega_i \leftarrow \omega_i + \delta\omega_i \tag{6}$$

$$\theta \leftarrow \theta + \delta\theta \tag{7}$$

The parameter κ is the ratio between the heat capacity of the feed and the path fluid. Also, the separation design function u_S may, in principle, be a continuous function, but here it is only allowed to be a point extraction just after each stage. The function is not subject to optimization but is based on data from the selected separation technology.

$$\delta\gamma = \gamma \sum s_i \omega_i \tag{8}$$

$$\delta\omega_i = (\gamma s_i \omega_i - \omega_i \delta\gamma)/(\gamma - \delta\gamma) \tag{9}$$

$$\delta\theta = c \tag{10}$$

$$\gamma \leftarrow \gamma - \delta\gamma \tag{11}$$

$$\omega_i \leftarrow \omega_i - \delta\omega_i \tag{12}$$

$$\theta \leftarrow \theta - \delta\theta \tag{13}$$

Here, $s_i \in [0,1]$ is the degree of separation of component i and is given as constants based on a more rigorous calculation of the separation, e.g. a flash calculation. The change in temperature after the separation will depend on the selected process of separation and is given as a constant c.

The model is made dimensionless, scaled relative to the make-up feed mass flow rate, W_0. All the design functions are bounded by maximum and minimum limits and are parameterized as piece-wise constant or piece-wise linear over each stage. They may also be chosen as fixed values, i.e. not to be optimized. In addition, state constraints are in general necessary to be included in any real design problem. A state constraint is, for example, a maximum temperature limit of the fluid along the path. The following design functions and parameters are included:

a. The total reaction volume V_R, is subject to optimization. The reaction volume is the total volume filled with a catalyst or the volume where the reaction takes place. The actual parameter to be optimized is the scaled parameter, $\sigma = V_R/W_0$.
b. The relative distribution of reaction volumes $\Delta\xi_i$ on the stages is subject to optimization. The actual parameters are the fraction of the total reaction volume, and the sum of all fractions must add up to unity, $\sum \Delta\xi_i = 1$.
c. The fluid mixing, u_M, on each stage is optimized, i.e. segregated flow, completely mixed, or something in between. The realization of fluid mixing of a tubular fixed bed reactor can be done by recycling the fluid around the beds. The fluid mixing will have an effect on both the reaction kinetics and the temperature profile.
d. Catalyst dilution, u_A, or distribution of catalyst concentration at each stage may be subject to optimization. The actual design function is the fraction of the maximum catalyst density available for reaction. The catalyst effectiveness factor is included in the design function. For the system studied here, u_A is kept constant.
e. The distribution of heat transfer area density, u_H, i.e. the heat transfer area over the reaction volume may be subject to optimization. The actual design function is $\beta = Ua/c_p$, with unit kg m^{-3} s^{-1}, where a is heat transfer area density, with dimension m^2 m^{-3}, U is the overall heat transfer coefficient and c_p is the average fluid heat capacity on a mass basis. Here, u_H is kept constant.
f. The coolant temperature distribution along the path, u_T, is subject to optimization.
g. The feed distribution along the path, u_F, is subject to optimization. In principle, the feed distribution can be continuous along the path, but here, only point-wise feeds in front of each stage are allowed.
h. The function u_S makes it possible to extract one or more chemical components between the stages. This function is not subject to optimization but is set based on knowledge of the selected separation technology and separation efficiency. For the system at hand, methanol and water will be removed between the stages and the obvious technique is by cooling and condensation.

The optimization problem is formulated as a feasible path optimization problem where the design functions are parameterized as piece-wise constant or piece-wise linear functions.

$$\max_{\mathbf{u} \in \mathscr{U}} J(\mathbf{x}, \mathbf{u}) \tag{14}$$

$$\frac{d\mathbf{x}}{d\xi} = \mathbf{f}(\mathbf{x}, \mathbf{u}), \quad \mathbf{x}(0) \in \{\mathbf{x}_{MUG}, \mathbf{x}_{Mix}\} \tag{15}$$

$$\mathbf{h}(\mathbf{x}, \mathbf{u}) = \mathbf{0} \tag{16}$$

$$\mathbf{g}(\mathbf{x}, \mathbf{u}) \le \mathbf{0} \tag{17}$$

Here, $\mathbf{u}$ is a vector of parameters describing the total reaction volume, volume distribution, and design functions that are selected to be optimized. If the path optimization is a once-through optimization, the initial state will be the make-up gas condition $\mathbf{x}_{MUG}$. However, when recycling of the tail gas is applied, the initial condition is determined by mixing the make-up gas with the recycled gas, $\mathbf{x}_{Mix}$. A set of equality constraints defining the mass balance of the mixing is added.

2.2. Reaction kinetics

There are several kinetic models available for commercial Cu/ZnO/Al_2O_3 catalysts. One of the most referenced models is one by Graaf et al. [11,12]. They developed the kinetics of three reactions.

$$CO + 2H_2 \overset{r_A}{\rightleftharpoons} CH_3OH \tag{18}$$

$$CO_2 + H_2 \overset{r_B}{\rightleftharpoons} CO + H_2O \tag{19}$$

$$CO_2 + 3H_2 \overset{r_C}{\rightleftharpoons} CH_2OH + H_2O \tag{20}$$

In their experimental work, they have varied the feed CO/CO_2 ratio from 0 to 2.7. Since the concentration span is relatively broad, the model is applicable for a feed gas consisting mainly of hydrogen and CO_2.

$$r'_A = k_A K_{CO}[f_{CO} f_{H_2}^{3/2} - f_{CH_3OH}/(f_{H_2}^{1/2} K_{p1})]/D \tag{21}$$

$$r'_B = k_B K_{CO_2}\left[f_{CO_2} f_{H_2} - f_{H_2O} f_{CO}/K_{p2}\right]/D \tag{22}$$

$$r'_C = k_C K_{CO_2}[f_{CO_2} f_{H_2}^{3/2} - f_{CH_3OH} f_{H_2O}/(f_{H_2}^{3/2} K_{p3})]/D \tag{23}$$

$$D = (1 + K_{CO} f_{CO} + K_{CO_2} f_{CO_2})(f_{H_2}^{1/2} + \left(K_{H_2O}/K_{H_2}^{1/2}\right) f_{H_2O}) \tag{24}$$

Here, r'_j is the reaction rate of reaction $j \in \{A, B, C\}$ with unit kmol s^{-1} kg$_{cat}^{-1}$, and f_i is the fugacity of component i in unit bar. All the estimated parameters are modeled with the Arrhenius type structure $\kappa = A\exp(\frac{-E}{RT})$, and the units are consistent with the rate expressions above Table 1.

For the path optimization method described above, it is necessary to convert the reaction rates from mass-specific to volume-specific rates. The rates are multiplied by the catalyst bulk density, $r_j = \rho_{bulk} r'_j$. The

Table 1
Estimated kinetic parameters from Graaf et al. [12]. The overall equilibrium constants are also given.

κ	A	E [J mol^{-1}]
k_A	$4.89 \cdot 10^{7}$	$1.130 \cdot 10^{5}$
k_B	$9.64 \cdot 10^{11}$	$1.529 \cdot 10^{5}$
k_C	$1.09 \cdot 10^{5}$	$0.875 \cdot 10^{5}$
K_{CO}	$2.16 \cdot 10^{-5}$	$-\ 0.468 \cdot 10^{5}$
K_{CO_2}	$7.05 \cdot 10^{-7}$	$-\ 0.617 \cdot 10^{5}$
$K_{H_2O}/K_{H_2}^{1/2}$	$6.37 \cdot 10^{-9}$	$-\ 0.840 \cdot 10^{5}$
K_{p1}	$1.6670 \cdot 10^{-13}$	$-\ 9.8682 \cdot 10^{4}$
K_{p2}	$1.1752 \cdot 10^{2}$	$3.9652 \cdot 10^{4}$
K_{p3}	$1.959 \cdot 10^{-11}$	$-\ 5.9030 \cdot 10^{4}$

catalyst bulk density is $\rho_{bulk} = 1170\ kg_{cat}\ m^{-3}$. The individual component reaction rates are $R_i = \sum_j \nu_{i,j} r_j$, where $\nu_{i,j}$ are the stoichiometric coefficients of component i in reaction j. The kinetic parameters are estimated with small particles with no mass transfer resistance, while in an industrial reactor, 4 mm pellets are used. The effectiveness factors η_j are approximately 0.8 for all three reactions. The design function u_A is the product of catalyst effectiveness and catalyst concentration/activity. The activity is relative to the estimated kinetics and a fresh catalyst is used. With a fresh catalyst and with no catalyst dilution or concentration, the maximum value of u_A is 0.8. In all cases studied here, the catalyst dilution function is set constant to a constant value, $u_A = 0.8$.

2.3. The methanol loop

A conventional Lurgi methanol synthesis loop, based on syngas from the reformation of natural gas, is with a one-stage reactor. The effluent gas from the reactor is cooled and water and methanol are condensed and separated from the unconverted syngas. The major part of the gas is recycled, while the rest is purged in order to prevent the inert concentration to become too high. The conversion per pass is limited by the equilibrium conversion.

There are five chemical components participating in the three reactions, Eqn. (18)–(20), of which only two are independent. Hence there are three reaction invariants. One of the reaction invariants can be formulated as the stoichiometric consumption ratio, $(R_{H_2} - R_{CO_2})/(R_{CO} + R_{CO_2}) = 2$. When the make-up gas stoichiometric mole number ratio, or modulus, $(y_{H_2} - y_{CO_2})/(y_{CO} + y_{CO_2})$ is two, the ratio inside the loop will remain two. If the make-up stoichiometric number ratio is slightly higher than two, the ratio inside the loop will be amplified depending on the recycle ratio. A high stoichiometric number ratio or hydrogen concentration is known to be beneficial for the reaction rates. For a make-up gas without any CO, the ratio $y_{H_2}/y_{CO_2} = 3$ is equivalent to a stoichiometric number ratio of two. A second reaction invariant is $R_{H_2O} = -R_{CO_2}$, the rate of water formation is equal to the rate of CO_2 consumption. Increasing the CO_2-conversion will also increase the water content. The third is more obvious, $R_{CH_3OH} = -R_{CO_2} - R_{CO}$.

The multi-stage concept with inter-condensation makes it possible to obtain much higher CO_2-conversion per pass. The water content will be kept low by removing water and methanol along the path. Removing the products, the equilibrium will also be shifted toward high conversion. Recycling unconverted CO_2 becomes less critical while recovering the excess hydrogen is important. A "superstructure" of the path optimization is depicted in Fig. 1.

In addition to the design functions described above, we will also analyze two options for the tail gas treatment after the last stage as shown in Fig. 1. .

1. Once-through path optimization, i.e. the make-up gas and the extra hydrogen feed are independent of the final tail gas. To recover the unconverted excess hydrogen from the tail gas, it is separated by using a pressure swing adsorption unit (PSA). From the PSA there is also an off-gas stream consisting of unconverted CO_2, CO, and inerts in addition to some hydrogen loss. A PSA is an appropriate separation technique as the product gas, hydrogen, will pass through the adsorption bed with a minor pressure loss and high purity. The recovered pure hydrogen will then be part of the extra hydrogen feed.

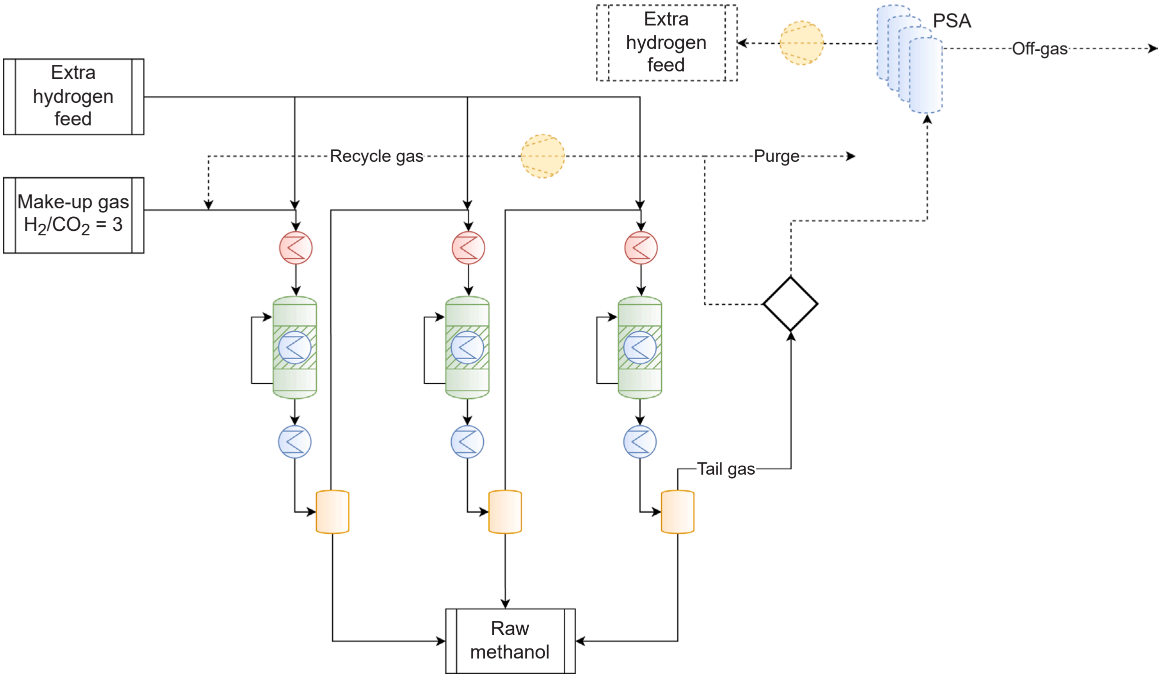

Figure 1. A "superstructure" of a three-stage methanol synthesis path. Two alternative options for the tail gas treatment; 1) once-through path optimization with purification of the tail gas with a pressure swing adsorption unit and 2) path optimization with recycling the tail gas without component separation. The number of stages is two or three. Fixed bed reactor with cooling is selected as reactor type. Recycling around the catalyst beds indicating that fluid mixing (dispersion) also is part of the optimization.

2. Recycle path optimization, i.e. by recycling a large fraction of the tail gas without any component separation. Typically 95% of the tail gas is recycled while the remaining 5% is purged in order to prevent too high inert built up. The extra hydrogen added in this case will naturally be considerably smaller as much hydrogen comes with the recycled gas. The recycle path optimization is with a priori unknown feed composition and flow rate, but these are calculated by a set of equality constraints defined by the mass balances around the loop.

Extra feeding of hydrogen is subject to optimization in both configurations. To increase the production of methanol, extra hydrogen is one of the key “handles” we have available, in addition to reaction volume. Therefore, much hydrogen will be in the tail gas, that needs to be recovered. For a PSA unit the loss of hydrogen will be proportional to the amount of adsorbed components, CO_2, CO, and inerts, since hydrogen is used to flush out the adsorbed/desorbed components. In configuration 2, the loss of hydrogen is given by the amount of hydrogen in the purge.

A commonly used methanol synthesis reactor type is a shell and tube boiling water reactor which is the type chosen here. The reactor has very good heat transfer properties due to boiling water on the shell side. Even though the exothermicity is relatively low, it is important to have good control of the reactor temperature, partly due to the sintering problem.

2.4. The objective function

An economic objective function, J, is constructed that reflects the cost effect of changing the design. All terms that are constant need not be included. The objective function should include the revenue of the product less the operating cost, minus the annualized capital cost of the investment. The make-up gas contains a stoichiometric ratio of $H_2/CO_2 = 3$, and since the flow is constant this cost need not be included in the objective function. The annualized capital cost ratio, ACCR, is approximately 10–30% per year. The cost of the reactor is assumed to be proportional to the reaction volume, aV_R.

$$J' = p_{CH_3OH} W_{CH_3OH} - \mathrm{ACCR} \cdot aV_R - c_{H_2} W_{H_2} \tag{25}$$

$$J'/p_{CH_3OH} = W_{CH_3OH} - w_1 V_R - w_2 W_{H_2} \tag{26}$$

$$J = J'/(p_{CH_3OH} W_0) = W_{CH_3OH}/W_0 - w_1 \sigma - w_2 u_F \tag{27}$$

Here, p_{CH_3OH} and W_{CH_3OH} are the price and the production rate of methanol, respectively. While W_{H_2} and c_{H_2} are the feed rate and the specific cost associated with the use of extra hydrogen.

The weight parameter, w_1, is the relative penalty of increasing the reaction volume. There are many uncertainties when estimating this value, and the value is estimated to be in the range $w_1 = 0.003 - 0.04$ kg m^{-3} s^{-1}. Values at the lower range of the interval tend to increase the volume unnecessarily to obtain high production. Rather, a value at the higher end of the interval is more likely to be of interest. With a value of $w_1 = 0.04$ kg m^{-3} s^{-1}, high production can be obtained with the least possible reaction volume.

The weight parameter, w_2, is the cost of adding extra hydrogen relative to the value of the product. Since most of the hydrogen is recovered and recycled only a fraction of the hydrogen is lost. There is, however, a cost of recovering, re-compressing, and recycling the hydrogen in addition to the lost hydrogen. The value of this parameter is also uncertain.

3. Results of the path optimization

The path optimization described above is used to generate several optimal designs by varying the weights, w_1 and w_2, the path constraints, and the number of stages. In the optimized designs presented here, there are several common design specifications that are applied in all or most cases:

- The objective function is maximized subject to a constraint on the temperature along the path being less than 270°C. This is because high temperatures will increase the catalyst sintering and deactivation. In one case the temperature constraint is reduced to 260°C.
- The total pressure is constant and equal to 82 bar in all cases.
- The heat transfer area density is kept constant in all stages and all cases $\beta = Ua/c_p = 35$ kg m^{-3} s^{-1}.
- The catalyst concentration is kept constant at 0.8 for all stages and all cases.
- The coolant temperatures at each stage can be optimized individually. In some cases they are. However, it is more practical to operate with a common coolant temperature and thus a common steam pressure.
- Since high per-pass conversion is possible with a multi-stage concept, a minimum CO_2-conversion of 95% per pass is applied in many cases.

There are also some results of the optimization that apply to all cases and need not be mentioned too many times:

- In all cases the optimal fluid mixing is segregated flow, i.e. fluid back-mixing is not optimal. The kinetics favors segregated flow.
- In all cases it is optimal to feed all the extra hydrogen solely to the first stage.
- The resulting temperature profiles are in all cases flat, i.e. the peak temperature is less than 10°C above the coolant temperature.

3.1. Configuration 1, once-through path optimization

Once-through path optimization is when the tail gas after the last stage is not recycled, i.e. the extra feed of hydrogen is independent of the tail gas composition. In reality, the major part of the hydrogen will be recovered in a separation unit and used as the extra feed of hydrogen. Table 2 shows several optimized cases. The feed of extra hydrogen is subject to optimization in all cases except in case 1.5 where no hydrogen is added. The total reaction volume, the distribution of volumes, and the coolant temperature are subject to optimization in all cases. Different values of the two weight parameters, w_1 and w_2, are explored.

The cases with the highest CO_2-conversion, cases 1.6 and 1.7, are with three stages and with no cost of adding extra hydrogen in addition to a low cost of increasing the reaction volume. The cases with low cost of the reaction volume, tend to give too large reaction volumes. This can be seen as idle volumes from the concentration profiles.

By increasing the cost of adding hydrogen, w_2, the amount of hydrogen is naturally reduced while the reaction volume is increased in order to obtain a desired CO_2-conversion. Fig. 2 shows the sensitivity of changing the parameter w_2 while keeping $w_1 = 0.04$. In all cases, a three-stage configuration is optimized with the same coolant temperatures in all stages and with constraints on the per pass conversion, $X_{CO_2} \geq 95\%$. To obtain a CO_2-conversion of at least 95% per pass, the total reaction volume is increased in order to reduce the required extra hydrogen addition. As can be seen from Fig. 2, the reaction volume increases quite rapidly when the extra hydrogen addition is reduced, by increasing the weight w_2. Furthermore, when the CO_2-conversion is on the constraint 95%, the optimal coolant temperature decreases as the reaction volume increase. The reason is, as the reaction volume increases the residence time increases and the conversion will be less dependent on the forward kinetics and more on the thermodynamic equilibrium conversion. Equilibrium conversion is favored by low temperatures. We also observe that compared to conventional syngas, the coolant temperature is somewhat higher as CO_2 is less reactive than CO.

Figure 3 shows the mass fraction concentration profile and the temperature along the path of case 1.9 from Table 2, where $w_1 = w_2 = 0.04$. As can be seen, the hydrogen concentration is very high and the intert is low. The extra hydrogen mass flow is 0.392 of the makeup gas on a mass basis. The molar H_2/CO_2 ratio is approximately 13 at the inlet

Table 2
Configuration 1, once-through path optimization. N_{st} is the number of stages, w_1, w_2 are the weights defined in the objective function, W_{H_2}/W_0 is the extra hydrogen feed over the make-up gas feed, and V_R/W_0 is the total reaction volume over the make-up gas feed. In some cases, the stages are with individual coolant temperatures while others are with uniform coolant temperatures as indicated by the temperature. The first 8 cases are without constraint on the CO_2-conversion and with no cost of the hydrogen addition, while the two last are with the constraint $X_{CO_2} \geq 95\%$.

Case	N_{st}	w_1	w_2	H_2 feed W_{H_2}/W_0	V_R/W_0 [m^3 s kg^{-1}]	Volume dist-ribution [%]	Coolant temp. [°C]	X_{CO_2}
1.1	2	0.04	0	1.020	2.603	55.0, 45.0	262, 262	92.87
1.2	2	0.04	0	0.991	2.683	47.5, 52.5	266, 253	92.84
1.3	3	0.04	0	0.667	2.316	40.2, 31.6, 28.2	263, 263, 263	96.97
1.4	3	0.04	0	0.631	2.360	36.6, 30.1, 33.3	265, 263, 254	96.86
1.5	3	0.04	0	0	1.446	33.3, 30.8, 35.9	266, 263, 259	54.98
1.6	3	0.003	0	0.828	5.689	26.4, 30.9, 42.7	264, 249, 231	99.67
1.7	3	0.003	0	0.912	6.128	42.5, 31.3, 26.2	247, 247, 247	99.73
1.8	3	0.04	0	0.346	2.231	53.7, 24.7, 21.6	262, 262, 262	93.53
1.9	3	0.04	0.04	0.392	2.413	53.8, 24.8, 21.4	262, 262,262	95.0
1.10	3	0.04	0.04	0.383	2.511	53.1, 23.5, 23.4	261, 262,257	95.0

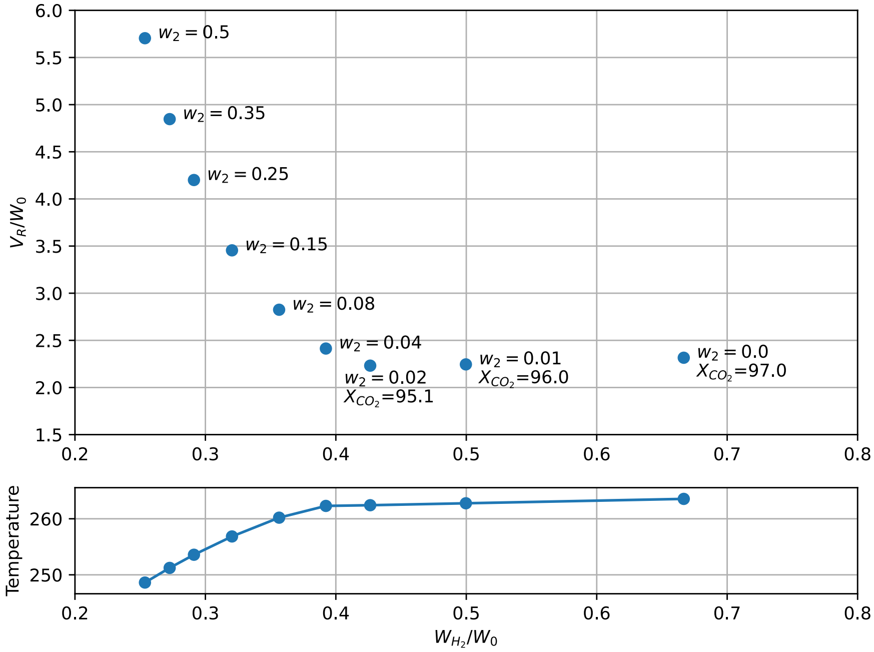

Figure 2. Sensitivity of changing the parameter w_2 while keeping $w_1 = 0.04$ with the once-through configuration. All points are optimized designs with three stages where the CO_2-conversion is constraint $X_{CO_2} \geq 95\%$. The six far left points are on the constraint conversion, $X_{CO_2} = 95\%$ while in the other three cases, the conversion is higher. The optimal coolant temperature is shown in the lower plot.

of the path and increases as the CO_2-conversion increases. The hydrogen outlet fraction is 98.3 mol%. There is some production of CO and the outlet mass fraction is 6.17%, equivalent to 0.54 mol%. The maximum water mass fraction after the first stage is approximately 14.4%, equivalent to 4.31 mol%.

3.2. Configuration 2, path optimization with recycle

Path optimization with recycling implies that the initial or feed condition of the model Eqn. (1) is not a priori known. A set of equality constraints, defining the initial condition as a set of non-linear equations, has to be added to the optimization.

Table 3 shows several optimized cases all with constraints on the CO_2-conversion, $X_{CO_2} \geq 95\%$. The split ratio, determining how much of the tail gas is recycled, is assigned the values 0.95 and 0.98.

All of the cases shown in Table 3 are with a maximum temperature constraint of 270°C, except case 2.12 which is 260°C. Cases 2.7 and 2.12 are otherwise the same.

Optimized cases with the recycle configuration 2 and with different values of the weight w_2 are shown in Fig. 4. Here, all the cases are with three stages and constraints on the CO_2-conversion, $X_{CO_2} \geq 95\%$. We see the same tendency as with the once-through configuration but with considerably less extra hydrogen feed.

The relative volume distribution, shown in Fig. 5, is with the same cases as shown in Fig. 4. As the total volume increases and extra hydrogen and temperature decrease, the first stage becomes relatively larger compared to the second and third stages. A possible explanation may be: With larger total volumes and lower temperatures, the first stage is allowed to approach closer to the equilibrium conversion by increasing the size of the first stage relative to the two last. On the contrary, with smaller total volumes and smaller residence times, the volume distribution becomes more even.

The concentration and temperature profiles along the path for case 2.7 with the recycle configuration are shown in Fig. 6. As expected, we see that the inert concentration is much higher than for the once-through configuration, but still not very high. The molar H_2/CO_2 ratio at the inlet of the path is approximately 21, which is higher than the once-through case. The fraction of hydrogen in the tail gas is approximately 93 mol%. The recycle ratio is 1.25. The inert and CO fractions at the outlet are 6.0 and 0.4 mol%, respectively. The maximum water mass fraction after the first stage is approximately 9.05% equivalent 2.37 mol %.

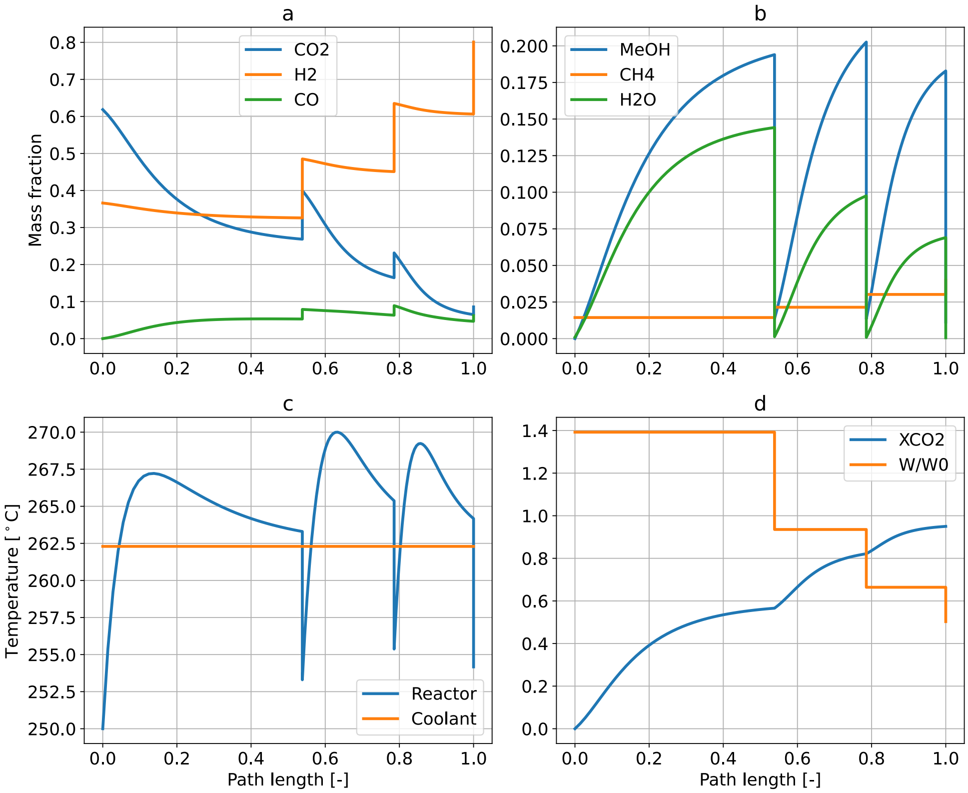

Figure 3. Configuration 1, the optimal Case 1.9 from Table 2, where the weights are $w_2 = 0.04$ and $w_1 = 0.04$. The coolant temperature is optimized but equal for all stages. The CO_2-conversion is on the minimum constraint, $X_{CO_2} = 95\%$. Plot a) shows the mass fractions of CO_2, H_2 and CO while plot b) shows the mass fractions of CH_3OH, CH_4 and H_2O. Plot c) shows the path temperature and the coolant temperature. Plot d) shows the CO_2-conversion and the relative mass flow W/W_0 along the path.

Table 3

Configuration 2, path optimization with recycle. N_{st} is the number of stages, w_1, w_2 are the weights defined in the objective function, W_{H_2}/W_0 is the extra hydrogen feed over the make-up gas feed, and V_R/W_0 is the total reaction volume over the make-up gas feed. Some cases are with uniform coolant temperatures while others are with individual coolant temperatures. All cases are with are with constraint on the CO_2 conversion, $X_{CO_2} \geq 95\%$. The last case, 2.12, is with a temperature constraint of 260˚C.

Case	N_{st}	w_1	w_2	Split ratio	H_2 feed W_{H_2}/W_0	V_R/W_0 [m^3 s kg^{-1}]	Volume dist-ribution [%]	Coolant temp. [˚C]	X_{CO_2}
2.1	2	0.04	0.04	0.95	0.0828	3.712	54.3, 45.7	266, 2.266	95.0
2.2	2	0.04	0.15	0.95	0.0828	3.797	57.2, 42.8	266, 266	95.0
2.3	3	0.04	0.50	0.95	0.0289	2.737	51.7,25.1,23.2	263,263,263	95.0
2.4	3	0.04	0.35	0.95	0.0303	2.634	49.8,26.0,24.2	263,263,263	95.0
2.5	3	0.04	0.25	0.95	0.0317	2.561	48.2,26.7,25.1	263,263,263	95.0
2.6	3	0.04	0.15	0.95	0.0337	2.483	46.0,27.7,26.3	264,264,264	95.0
2.7	3	0.04	0.04	0.95	0.0382	2.403	41.6,29.7,28.7	264,264,264	95.0
2.8	3	0.04	0.01	0.95	0.0406	2.389	39.4,30.6,29.9	264,264,264	95.0
2.9	3	0.04	0.0	0.95	0.0416	2.387	38.5,31.1,30.4	264,264,264	95.0
2.10	3	0.04	0.04	0.98	0.0193	2.749	39.0,30.5,30.5	265,265,265	95.0
2.11	2	0.04	0.04	0.98	0.0381	4.091	52.8, 47.2	267,267	95.0
2.12	3	0.04	0.04	0.95	0.0365	2.963	40.9, 30.6, 28.5	255,255,255	95.0

4. Realisation of a design concept

The applied path optimization method is based on simplified models and assumptions. The method can be viewed as a shortcut method for generating the optimal configuration. From the path optimization, we will obtain the reaction volumes, V, and the volumetric flow rates, q, of each stage and thus the residence times. The geometric design of the reactor is not given by the path optimization e.g. the length and diameter of tubes. These details are essential with respect to the overall heat transfer, U, and pressure drop, ΔP. The overall heat transfer is a lumped parameter given by the resistance on the inside and the outside of the wall and will have a pronounced effect on the temperature profile. So far, we have only set a target of the lumped parameter $\beta = Ua/c_p$. If the reactor consists of tubes filled with catalysts, the specific heat transfer area is given by the tube diameter, $a = 4/d$. Furthermore, if the heat transfer resistance is dominated by the inside wall heat transfer coefficient, the overall heat transfer coefficient is very much given by the superficial gas velocity, v. The gas velocity is a parameter we have to “guess" and iterate so as to have reasonable values of U and ΔP. The number of tubes is given by the volumetric flow rate and the superficial gas velocity, $N_t = q/(\frac{\pi}{4}d^2v)$ and the tube length is given by the reaction volume, $L_t = V/(\frac{\pi}{4}d^2N_t)$. For practical reasons, the tube length of each stage should be of equal length. If the tube length of each stage becomes slightly different, make them equal so that there will be no problem with overall heat transfer or pressure drop. Instead, the gas velocity may change somewhat from stage to stage. Similar engineering calculations can be made with other geometries.

4.1. *Design basis*

The make-up gas consists of 1.6% inert on a dry basis, here taken to be methane, and with a H_2/CO_2 ratio of 3. There is a small amount of water and no CO. The extra hydrogen feed is considered to be pure

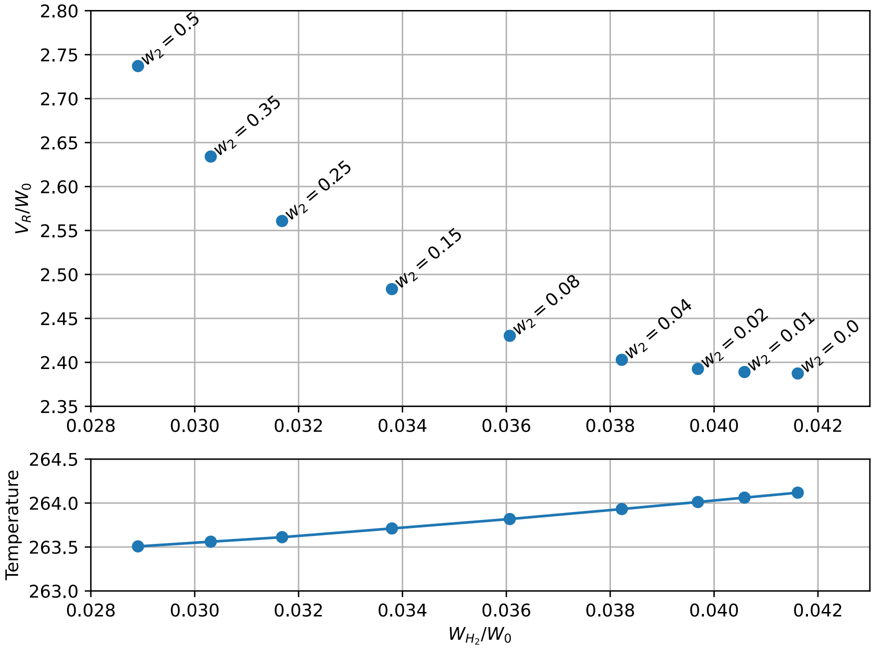

Figure 4. Sensitivity of changing the parameter w_2 while keeping $w_1 = 0.04$ with the recycle configuration. All points are optimized designs with three stages where the CO_2-conversion is on the constraint, $X_{CO_2} = 95\%$. The optimized coolant temperature, which is equal for all stages, is shown in the lower plot.

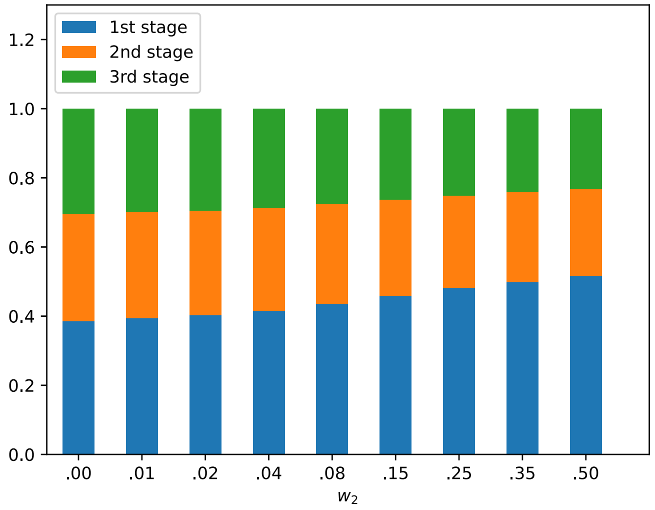

Figure 5. The relative volume distribution of the three-stage cases with tail gas recycling.

hydrogen.

The total capacity of a methanol plant based on renewable energy is not likely to be very large due to the limited availability of renewable energy. A relatively large plant chosen here is around 10 t h^{-1} of methanol. Let the make-up gas flow rate be 18 t h^{-1} which corresponds to $W_0 = 5.0$ kg s^{-1}. From the stoichiometry of Eqn. (20), 18 t h^{-1} of make-up gas can at the maximum produce $18 \times 32/50 = 11.52$ t h^{-1} methanol.

4.2. Heat integration

By limiting the heat integration to the cold and hot streams available in the methanol synthesis, the heat integration becomes quite straightforward. For each stage, a feed-effluent heat exchanger (interchanger) and an external cooler are applied. By matching feed and effluent streams of the same stage, the total flow heat capacity is about the same.

4.3. Verification

Promising configurations should be verified through a more rigorous simulation where the heat transfer coefficients are calculated along the reactor length. On the tube inside the Nusselt number (N_{Nu}) is calculated based on the particle Reynolds number (N_{Re}) and the Prandtl number (N_{Pr}).

$$N_{\mathrm{Nu}} = 1.60 N_{\mathrm{Re}}^{0.510} N_{\mathrm{Pr}}^{0.333} \tag{28}$$

On the tube outside, where we have boiling water, the heat transfer coefficient is very good and is set to $h_o = 1.0$ kW m^{-2} K^{-1}. The overall heat transfer will decrease along the length of the tube mainly because the gas velocity decreases. The pressure drop of the fixed bed is calculated based on Ergun's equation.

Two of the generated designs are implemented in the simulation software Aspen Hysys for more accurate calculations. The same kinetic model described above is applied. The results of the simulations of case 1.9 of the once-through configuration and case 2.7 of the recycle configuration are compared in Table 4. These two are selected because they have reasonable reaction volumes and hydrogen feeds.

A surprising observation is that case 2.7 generates less duty from the reactor even if the methanol production is higher than case 1.9. The heat duty from the reactors is proportional to the integral of the temperature difference between the gas and the coolant along the path length. The coolant temperature of case 2.7 is 264°C, while for case 1.9 it is 262°C. This explains the higher duty of case 1.9. In all cases the temperature profile is flat, i.e. the peak temperature is not much higher than the coolant temperature. This fact explains why the heat duty from the reactors is small compared to the duties of the coolers and the interchangers. It is not desirable to have too much duty on the coolers since most, not all, of the energy extracted from the coolers is lost energy while the steam produced in the reactor is at a higher temperature and more useful.

A possible way of improving the heat distribution is to reduce the reactor temperature. Less thermal energy will be carried by the effluent gas. A new path optimization is made with a path temperature constraint of 260°C. The rigorous simulation of case 2.12 is given in Table 5. The total reactor size increases from 12 to 14.8 m^3, with more steam

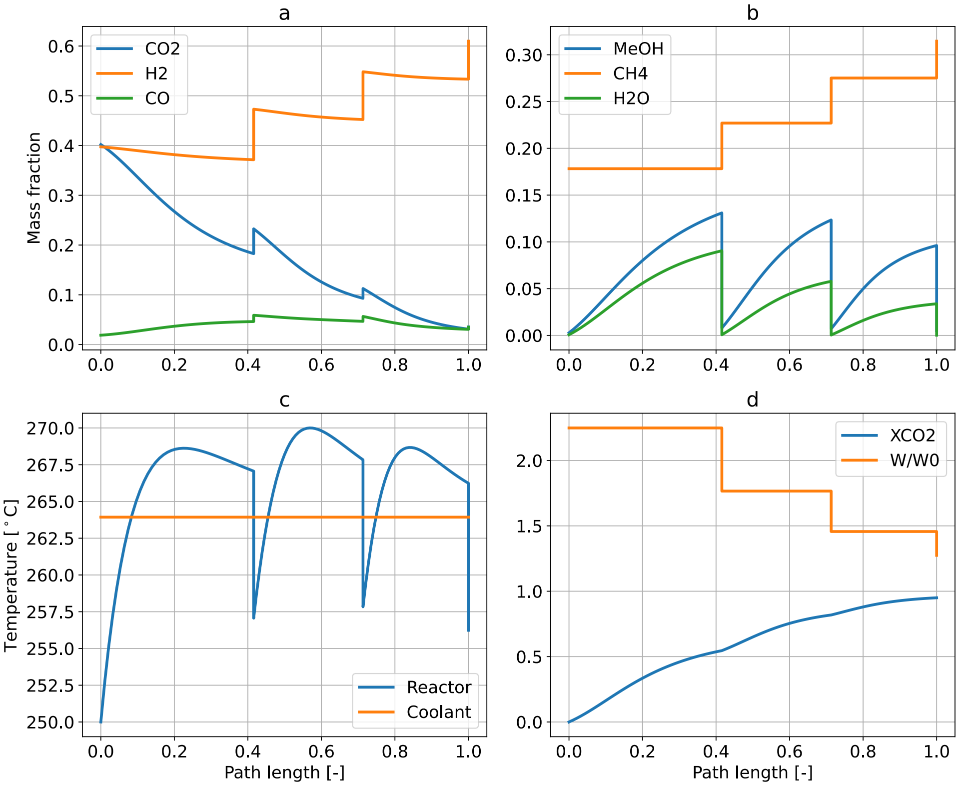

Figure 6. Plots showing the result of case 2.7 with configuration 2 recycling of the tail gas and with $w_2 = 0.04$ and $w_1 = 0.04$. Plot a) shows the mass fractions of CO_2, H_2 and CO while plot b) shows the mass fractions of CH_3OH, CH_4 and H_2O. Plot c) shows the path temperature and the coolant temperature. Plot d) shows the CO_2-conversion and the relative mass flow rate W/W_0 along the path.

produced and less external cooling, and the methanol production is slightly larger. If the maximum temperature is reduced even more, the reaction volume will increase quite rapidly as the conversion constraint is to be obtained.

4.4. Energy efficiency

Based on a rigorous model of case 2.12, implemented in Aspen Hysys, a simplified energy efficiency of the methanol synthesis can be calculated. The efficiency of the electrolyzers is not included, and

Table 4
Rigorous simulation of the once-through case 1.9 and the recycle case 2.7. The total volume is about the same, while the amount of added hydrogen is very different. The recycle ratio of case 2.7 is less than 1.25.

Case	Parameter	1st stage	2nd stage	3rd stage	Total
1.9	Reaction volume [m^3]	6.49	2.99	2.59	12.07
	Number of tubes	1723	792	686	3201
	Active tube length [m]	3.0	3.0	3.0	9.0
	Pressure drop [kPa]	12.32	34.40	30.86	77.58
	Peak temperature [°C]	270	270.5	268	
	Peak water fraction [mol%]	4.3	2.2	1.2	
	Coolant temperature[°C]	262	262	262	
	X_{CO_2} per pass	56.24	57.50	68.65	94.17
	Extra H_2 feed [kg h^{-1}]	7054	0	0	7054
	Methanol production [t h^{-1}]	4.49	3.08	1.95	9.52
	Heat duty from reactor [MW]	1.35	1.19	0.75	3.29
	Duty interchangers [MW]	7.22	7.51	6.78	21.51
	Duty coolers [MW]	5.68	2.47	1.53	9.68
2.7	Reaction volume [m^3]	5.00	3.57	3.45	12.01
	Number of tubes	1988	1422	1371	4781
	Active tube length [m]	2.0	2.0	2.0	6.0
	Pressure drop [kPa]	18.75	26.91	23.29	68.95
	Peak temperature [°C]	270	271	269	
	Peak water fraction [mol%]	2.3	1.3	0.7	
	Coolant temperature[°C]	264	264	264	
	X_{CO_2} per pass	52.76	56.01	65.87	92.91
	Extra H_2 feed [kg h^{-1}]	687.3	0	0	687.3
	Methanol production [t h^{-1}]	5.20	3.56	2.32	11.08
	Heat duty from reactor [MW]	0.79	0.71	0.34	1.84
	Duty interchangers [MW]	14.41	14.71	13.87	42.99
	Duty coolers [MW]	6.87	3.53	2.41	12.81

Table 5
Rigorous simulation of case 2.12. This case is similar to case 2.7 except that the maximum allowed temperature is 260°C.

Case	Parameter	1st stage	2nd stage	3rd stage	Total
2.12	Reaction volume [m^3]	6.06	4.53	4.22	14.82
	Number of tubes	1608	1203	1120	3931
	Active tube length [m]	3.0	3.0	3.0	9.0
	Pressure drop [kPa]	39.16	50.92	46.60	136.68
	Peak temperature [°C]	261.5	262	260	
	Peak water fraction [mol%]	2.4	1.4	0.7	
	Coolant temperature[°C]	255	255	255	
	X_{CO_2} per pass	52.78	58.66	69.60	94.06
	Extra H_2 feed [kg h^{-1}]	652.2	0	0	652.2
	Methanol production [t h^{-1}]	5.30	3.62	2.19	11.11
	Heat duty from reactor [MW]	1.64	1.39	0.89	3.92
	Duty interchangers [MW]	13.72	14.05	13.19	40.96
	Duty coolers [MW]	6.21	2.89	1.71	10.81

neither is the energy consumption of compressors. The higher heating value (HHV) of the makeup gas at 82 bar is 88.5 MW, while for the extra hydrogen feed, HHV is 25.4 MW. The higher heating value of the produced methanol is 70.9 MW and the purge is 32.0 MW. If we consider the purge as lost energy, the energy efficiency is approximately 62%. However, if we recover most of the hydrogen in the purge, say 20 MW, by using a PSA unit, the energy efficiency is close to 80%. The major part of the energy loss in the synthesis is through the coolers.

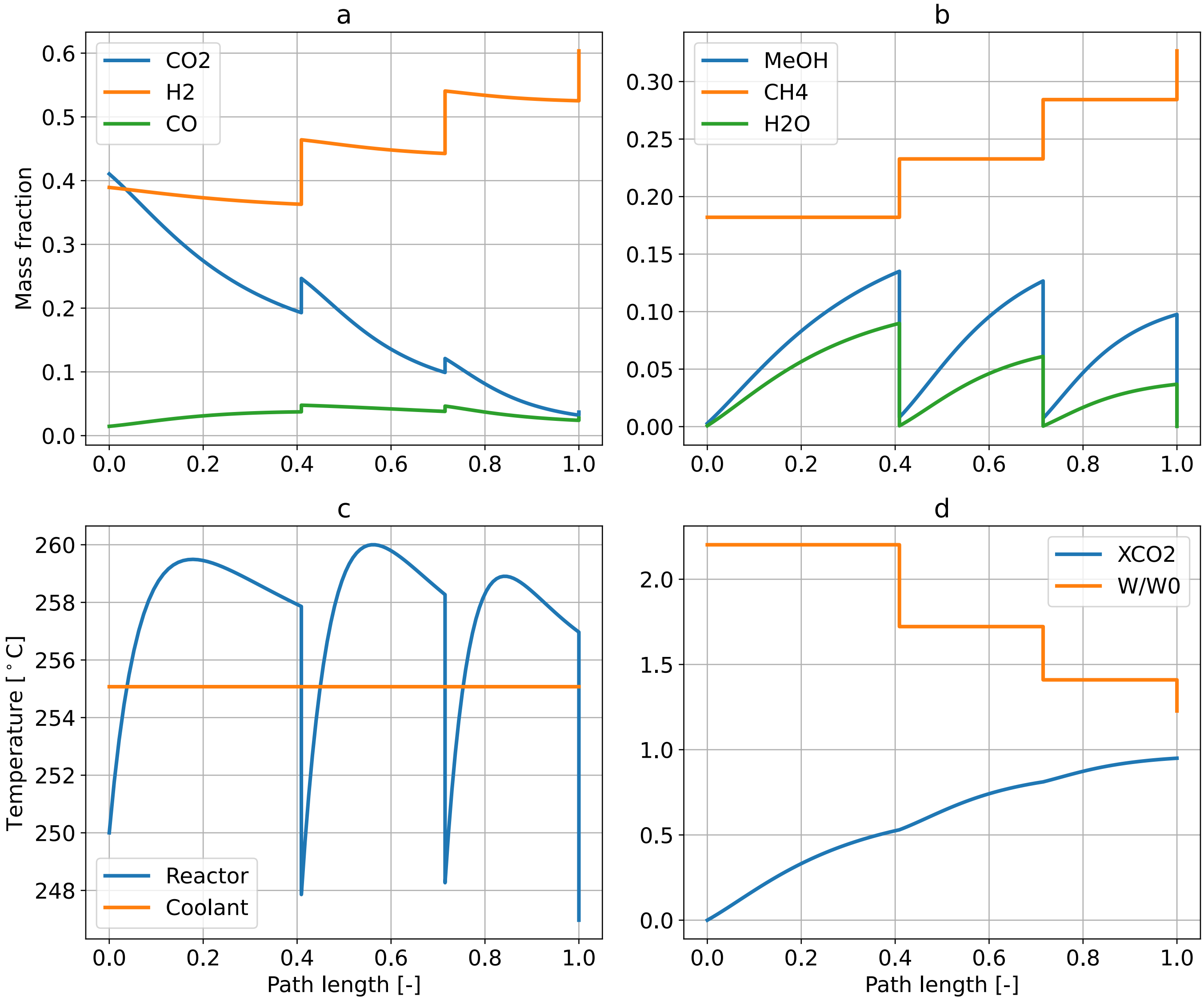

Figure 7. Plots showing the results of case 2.12 with $w_2 = 0.04$ and $w_1 = 0.04$. This is the same as case 2.7, except that the maximum temperature constraint is 260°C. Plot a) shows the mass fractions of CO_2, H_2 and CO while Plot b) shows the mass fractions of CH_3OH, CH_4 and H_2O. Plot c) shows the path temperature and the coolant temperature. Plot d) shows the CO_2-conversion and the relative mass flow W/W_0 along the path.

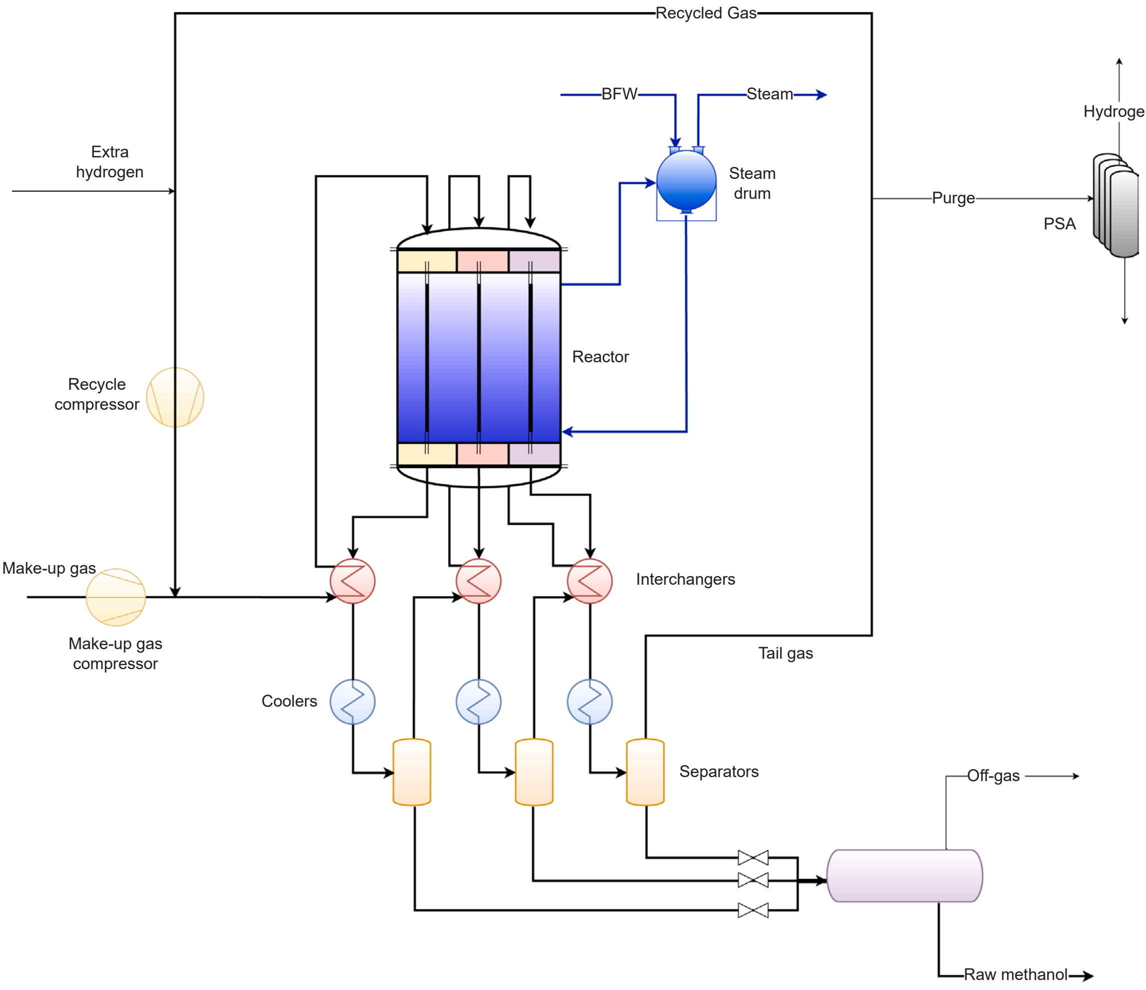

Figure 8. A three-stage optimized design with recycle and with all stages in one shell.

4.5. *Sintering effects*

From Fig. 7, showing the concentration and temperature profiles when the maximum path temperature is set to 260°C, we read the maximum water mass fraction is approximately 9.0% equivalent to 2.4 mol%. Compared with a one-stage methanol reactor based on conventional syngas from natural gas reforming, the maximum water concentration at the outlet is approximately 2.3 mol% with the same total pressure. A conventional syngas contains 21 mol% CO, 8.2 mol% CO_2, 69.1 mol% H_2, 0.1 mol% H_2O, and 1.6 mol% CH_4. The maximum water pressures are practically equal. The temperature where the peak water pressure is located is also comparable. This is a strong indication that the sintering effect will not be more pronounced with a staged CO_2 hydrogenation process than a methanol synthesis with conventional syngas.

4.6. *The proposed design*

Comparing the once-though case 1.9 with the recycled case 2.7 both require about the same reactor volume. The major difference is that the former requires a PSA unit to separate a large tail gas stream. Since the per-pass conversion is high, the recycling of the tail gas and the increased inert concentration do not affect the reaction volume much. The recycle ratio is about 1.25. The methanol production of case 2.7 is also somewhat larger. Therefore case 2.7 is considered to be a better alternative.

Comparing cases 2.7 and 2.12, both with recycle, the latter is operated at a lower temperature and therefore the reaction volume is somewhat larger. The distribution of heat duties is better with case 2.12 as more steam is produced and less external cooling is required. Of these two, 2.12 is considered a better alternative.

The purge gas of case 2.12 consists of about 92–93% hydrogen. All the extra hydrogen feed, which is surplus hydrogen, ends up in the purge. Compared to the tail gas of case 1.9, the purge of case 2.12 the flow rate is ca 1/10 in magnitude. It will therefore be much less expensive to invest in a PSA to recover the hydrogen from the purge than from the tail gas.

Figure 8 shows how the final design might look like. All three stages are located in one shell, with the same coolant temperature for all tubes. The heat interchangers and the coolers handle large heat duties, but there is condensation taking place in all of them so the overall heat transfer is good.

The outer tube diameter is 4 cm. With 3931 tubes arranged in a triangular pitch and with a pitch distance of 5 cm, the bundle of tubes would be ca 3.25 m. The steam pressure is 42.5 bar. The steam production is 8.2 t h^{-1}.

5. Discussion

The aim of this study is to apply a systematic staging method to design a process for the direct hydrogenation of CO_2 to methanol with the use of existing commercial catalysts. Since CO_2 produces more water than conventional syngas, it is more prone to catalyst sintering and deactivation. With a multi-stage reactor concept with inter-condensation, it is possible to obtain high conversions per pass and lower the water pressure to an acceptable level. High conversion per pass results in much less recycled gas and recycle compression in addition to lower inert concentration. The inert concentration of the recycled gas is only 6.2 mol%. For case 2.12, the maximum water fraction after the first stage is 2.4 mol%. For a conventional methanol loop and a conventional syngas, the maximum water fraction is 2.3 mol%, which is practically the same. In the once-though case 1.9, the water fraction is 4.3 mol%. The main disadvantage of the multi-stage design, compared to a traditional design, is that there will be several more heat exchangers and separators.

The optimal fluid mixing structure is segregated flow. The kinetics favors segregated fluid flow for all three stages. If the heat release rate has been greater than the heat transfer rate, a temperature runaway may occur and fluid back-mixing will level out any excessive temperature peaks. This is not the situation in any of the cases. The reaction heat is also moderate compared to normal syngas.

The rigorous simulations are more accurate than the models applied in the path optimization method. However, the deviations are not very large. The CO_2-conversion is slightly lower with the rigorous model, which may be explained by more accurate pressure drop calculations. Also, a more accurate heat transfer calculation may explain the small deviation of the peak temperatures.

With the recycle configuration and high conversion per pass, the recycle ratio is relatively small. The increased inert concentration with recycling does not imply a higher reaction volume than the once-through configuration.

The cases with no cost of adding extra hydrogen in Table 2, illustrate that by adding much hydrogen the conversion of CO_2 can be almost 100% even at moderate volumes.

This study is limited to methanol synthesis only. Neither hydrogen and CO_2 production, compression nor raw methanol separation is considered here. By considering the entire plant more extensive heat and mass integration will be possible, as reported by Lacerda de Oliveira Campos et al. [7]. Some heat from the coolers, though at low temperatures, may be recovered. However, heat integration and techno-economic analysis of the system may be topics for a separate study.

6. Conclusion

Direct hydrogenation of CO_2 to methanol with the use of hydrogen produced from renewable energy is a promising route for greenhouse gas emission reduction. In the methanol economy, Olah [13] suggests that methanol will be used 1) as energy-storage material, 2) as a fuel, and 3) as a feedstock to synthesize hydrocarbons and other products.

The hydrogenation of CO_2 to methanol produces water and since commercial methanol catalysts tend to deactivate faster in the presence of water, a process concept based on multi-stage reactors with inter-condensation is investigated. This concept is also suggested by others [6–8]. Here, based on a reaction kinetic model, a path optimization method is applied for the systematic staging of the process. Several design functions and variables, such as fluid mixing, hydrogen feed, coolant temperature, size, and distribution of reaction volumes are subjected to optimization of an economic objective function. The production of methanol is maximized with the least possible reaction volume cost and extra hydrogen cost. The optimization is constrained by a maximum allowed temperature along the path and a minimum CO_2-conversion of 95% per pass. Since the cost parameters of extra hydrogen and reaction volume are uncertain, their sensitivities in addition to the number of stages are studied. Several optimal designs are generated. A three-stage configuration with recycling of the tail gas is found to be a good solution. The water pressure and the temperature are similar to a one-stage reactor based on conventional syngas, indicating that the catalyst deactivation rate is likely to be equally low.

Declaration of Competing Interest

The authors declare that they have no known competing financial interests or personal relationships that could have appeared to influence the work reported in this paper.

Data Availability

No data was used for the research described in the article.

References

[1] B.D. Patterson, F. Mo, A. Borgschulte, M. Hillestad, F. Joos, T. Kristiansen, S. Sunde, J.A. van Bokhoven, Renewable CO_2 recycling and synthetic fuel production in a marine environment, Proc. Natl. Acad. Sci. USA 116 (25) (2019) 12212–12219, https://doi.org/10.1073/pnas.1902335116.

[2] S.G. Jadhav, P.D. Vaidya, B.M. Bhanage, J.B. Joshi, Catalytic carbon dioxide hydrogenation to methanol: a review of recent studies, Chem. Eng. Res. Des. 92 (11) (2014) 2557–2567. ⟨https://doi.org/10.1016/j.cherd.2014.03.005.https://www.sciencedirect.com/science/article/pii/S0263876214001282⟩.

[3] M. Ren, Y. Zhang, X. Wang, H. Qiu, Catalytic hydrogenation of CO_2 to methanol: a review, Catalysts 12 (4) (2022), https://doi.org/10.3390/catal12040403.

[4] P. König, H. Göhna, Process of producing methanol 1997. ⟨https://patents.google.com/patent/US5631302A/en⟩.

[5] A. Bansode, A. Urakawa, owards full one-pass conversion of carbon dioxide to methanol and methanol-derived products, J. Catal. 309 (2014) 66–70, https://doi.org/10.1016/j.jcat.2013.09.005.

[6] F. Samimi, M.R. Rahimpour, A. Shariati, Development of an efficient methanol production process for direct CO_2 hydrogenation over a $Cu/ZnO/Al_2O_3$ catalyst, Catalysts 7 (11) (2017), https://doi.org/10.3390/catal7110332.

[7] B. Lacerda de Oliveira Campos, K. John, P. Beeskow, K. HerreraDelgado, S. Pitter, N. Dahmen, J. Sauer, A detailed process and techno-economic analysis of methanol synthesis from H_2 and CO_2 with intermediate condensation steps, Processes 10 (8) (2022), https://doi.org/10.3390/pr10081535.

[8] S. Haag, C. Drosdzol, B. Williams, V. Peña, N. Palauschek, M. Wilken, A. Günther, V. Gronemann, A. Roesch, Recent developments in methanol technology by air liquide for CO_2 reduction and CO_2 usage, Chem. -Ing. -Tech. 94 (11) (2022) 1655–1666, https://doi.org/10.1002/cite.202200061.

[9] T. Oelmann, T. Schuhmann, M.G. Air, L. Engineering, A New Reactor Concept for Conversion of CO_2 to Methanol Conventional Methanol Technology Methanol Developments at Air Liquide CO2-to-MeOH (2020).

[10] M. Hillestad, Systematic staging in chemical reactor design, Chem. Eng. Sci. 65 (10) (2010), https://doi.org/10.1016/j.ces.2010.02.021.

[11] G.H. Graaf, E.J. Stamhuis, A.A. Beenackers, Kinetics of low-pressure methanol synthesis, Chem. Eng. Sci. 43 (12) (1988) 3185–3195, https://doi.org/10.1016/0009-2509(88)85127-3.

[12] G.H. Graaf, H. Scholtens, E.J. Stamhuis, A.A. Beenackers, Intra-particle diffusion limitations in low-pressure methanol synthesis, Chem. Eng. Sci. 45 (4) (1990) 773–783, https://doi.org/10.1016/0009-2509(90)85001-T.

[13] G.A. Olah, Beyond oil and gas: the methanol economy, Angew. Chem. - Int. Ed. 44 (18) (2005) 2636–2639, https://doi.org/10.1002/anie.200462121.